Path-Averaged Measurements of Rain Rate and Raindrop Size Distribution Using a Fast-Response Optical Sensor

TING-I WANG, K. B. EARNSHAW AND R. S. LAWRENCE

NOAA/ERL/Wave Propagation Laboratory, Boulder, CO 80302

(Manuscript received 7 November 1978, in final form 1 February 1979)

ABSTRACT

Path-averaged terminal velocity distribution of raindrops is determined from the temporal covariance function of signals from two vertically spaced linear optical detectors that respond to raindrop-induced amplitude scintillations of a projected laser beam. The known monotonic relationship between drop size and terminal velocity permits the measured velocity distribution to be converted to path-averaged drop-size distribution and, in turn, to rain rate. The large capture area of the measurements over a 200 m path allows drop-size distribution to be measured in short time intervals. We present measurements of path-averaged rain rate and raindrop size distribution made at 42 s intervals. The terminal velocity distribution during a storm that contained a mixture of rain and hail clearly shows the two-component nature of the precipitation.

1. Introduction

Several investigations of optical and infrared wave transmission through precipitation (Atlas, 1953; Arnulf and Bricard, 1957; Wilson and Penzias, 1966; Chu and Hogg, 1966, 1968; Atlas and Ulbrich, 1974, 1976; Hogg and Chu, 1975) suggest that path-averaged rain parameters may be deduced from line-of-sight attenuation measurements. Such line-averaged optical measurements significantly reduce the random fluctuations noted in rain rate measured by such point sensors as raingages. We have developed a rain-measuring technique that uses the rainfall-induced irradiance (or amplitude) scintillations of a laser beam (Wang and Clifford, 1975; Wang and Lawrence, 1977; Wang *et al.*, 1977, 1978) instead of the attenuation of the beam. This technique measures not only the path-averaged rain rate but also the drop-size distributions.

For a plane wave incident on a spherical raindrop (see Fig. 1) the scattered field can be approximated by two components: the field induced by diffraction of the sharp boundary of the drop and the light passing through the water drop (Van De Hulst, 1957). The transmitted field is much weaker than the diffractive field if we assume that the wavelength of the incident wave is much shorter than the radius of the drop (a reasonable assumption in optical and infrared band), and that the change of refractive index from unity is not small (i.e., $ka \gg 1$ and $ka\Delta n \gg 1$, where k is the wavenumber, a the radius of the drop, and $1+\Delta n$ the refractive index of water). Thus the total scattered field is approximately equal to the diffractive field. The scattered field can be considered as a spherical wave emitted from the center of the raindrop because we are only interested in the far-field solution (where the drop radius is much less than the Fresnel zone size, i.e., $a \ll (\lambda x)^{\frac{1}{2}}$, where x is the distance between the drop and the receiver and the transverse coordinate is much less than the longitudinal coordinate). The interference at the receiving plane, caused by the incident plane wave and the scattered spherical wave, gives the fine phase fringes shown in Fig. 1. The envelope of the interference pattern is the well-known Airy diffraction pattern of a sphere. The result was confirmed by photographing the signal detected by a point photodetector at a distance of 18 m from laboratory-produced falling water drops illuminated by a collimated laser beam (Fig. 2). Two succeeding patterns are shown in Fig. 2; the left pattern is induced by a small drop with a small amplitude scintillation and a wide scattering angle, and the right pattern is induced by a larger drop.

We obtain the path-averaged drop-size distributions and rain rates by observing the movement of the scintillations induced by falling raindrops randomly located along an optical path. A collimated laser beam illuminates two detectors placed with a vertical separation z_0 (see Fig. 3). We correlate the signals of raindrop-induced scintillations detected by the detectors to obtain the time-lagged cross-correlation function for different time lags τ. For a specified time lag τ, only those drops with terminal velocity v in the vicinity of z_0/τ will contribute to the correlation function, whereas the contribution for slower or faster drops is statistically negligible. By measuring the correlation at different time lags we obtain the path-averaged terminal velocity distribution of raindrops. Assuming a known monotonic relationship between a raindrop's size and its terminal velocity (Gunn and Kinzer, 1949), we can convert the

velocity distribution to the path-averaged drop-size distribution and then to rain rate.

2. Time-lagged cross-covariance function

Consider a plane wave traveling in the x direction and scattered by randomly located raindrops. If we assume that the raindrops are spherical and that the wavelength λ of the incident wave is much smaller than the radius a of the raindrop, the far-field time-lagged cross-correlation function of the amplitude scintillation observed by two line-detectors with a vertical separation z_0 has been given by Wang *et al.* (1977) as

$$C_\chi(z_0,\tau)=4.1\times10^{-16}z_0^2l^{-1}\tau^{-3}\left[g(z_0/\tau)+\frac{z_0}{\tau}\frac{g'(z_0/\tau)}{2}\right]\times\int_0^L dx h(x)P(a',x)$$

$$\approx\overline{P(a')}\tau^{-3}\left[g(z_0/\tau)+\frac{z_0}{\tau}\frac{g'(z_0/\tau)}{2}\right]. \quad (1)$$

In Eq. (1) τ is the time delay, l the length of the line detectors which are extended in the horizontal direction, L the pathlength, $h(x)$ the total rain rate (mm h^{-1}) at path-position x,

$$a'=2.5\times10^{-5}z_0^2\tau^{-2}g(z_0/\tau), \quad (2)$$

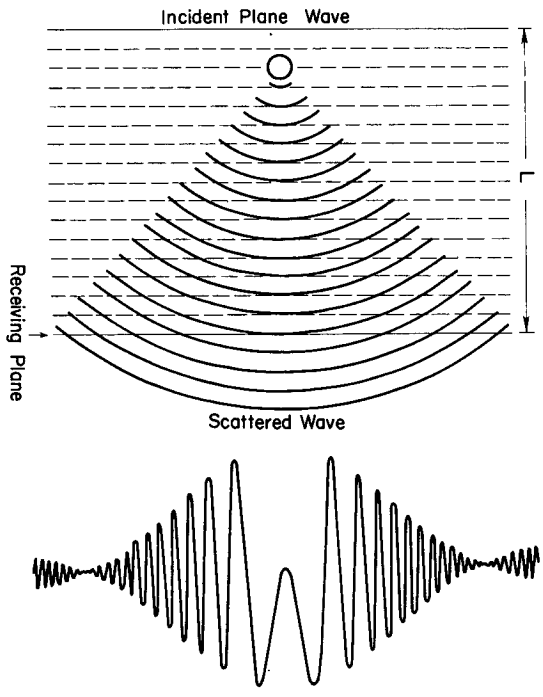

FIG. 1. The interference pattern induced by a spherical raindrop. The fine fringes are caused by the phase interference of the incident wave and scattered wave. The envelope of the interference pattern is the Airy diffraction pattern of a sphere.

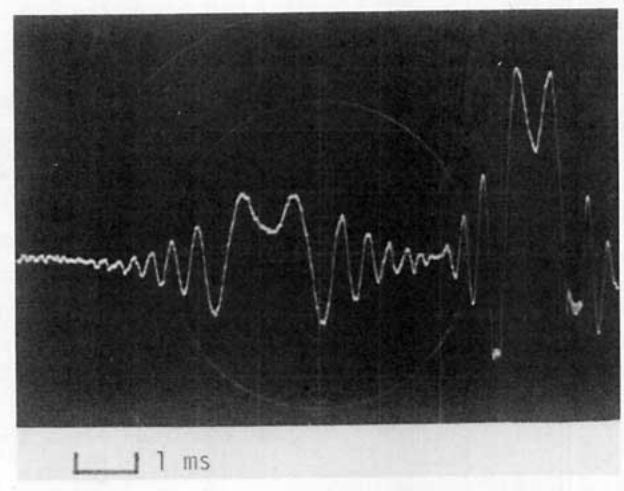

FIG. 2. The signal detected by a point photo-detector at a distance 18 m from laboratory-produced falling water drops illuminated by a collimated laser beam. The left-hand pattern was produced by a small drop and has a small amplitude but a wide scattering angle, the right-hand pattern was produced by a larger drop.

and $\overline{P(a')}$ is the path-averaged probability-density function of raindrop size. To obtain Eq. (1), we used the relationship between the raindrop radius and its terminal velocity given by

$$g(v)v^2=4\times10^4a, \quad (3)$$

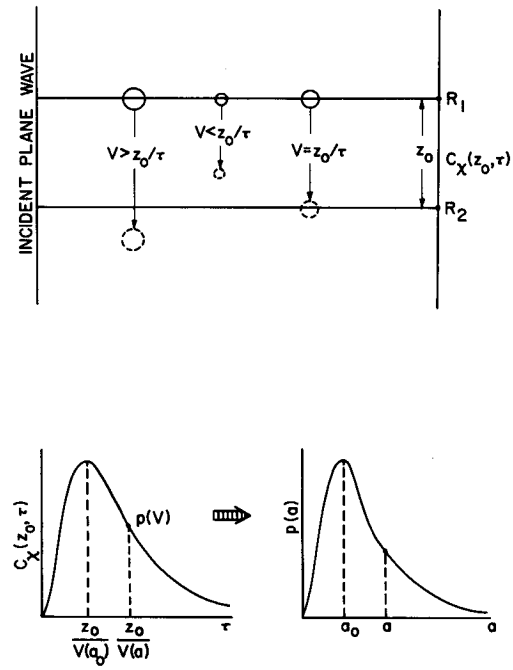

FIG. 3. For an incident plane wave, two horizontal detectors are placed with a vertical separation z_0. The time-lagged correlation function of the signals detected by the two detectors yields the terminal velocity distribution of raindrops, and this can be converted to drop size distribution for a known monotonic relationship between a raindrop's size and its terminal velocity.

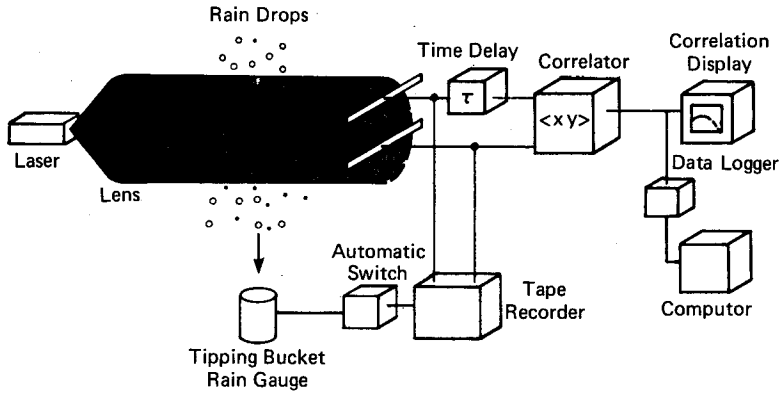

FIG. 4. Schematic diagram of a prototype optical rain sensor.

where $g(v)=2c$, c is the drag coefficient given by Gunn and Kinzer (1949), and $g'(v)$ denotes the derivative of $g(v)$ with respect to v. Here a is in meters and v is in meters per second.

The path-averaged rainfall rate $\bar{h}$ is obtained by integration over all sizes. If we multiply Eq. (1) by τ^3 and integrate over a', we obtain

$$\bar{h}=\frac{1.22\times10^{11}l}{L}\int_0^\infty d\tau C_\chi(z_0,\tau). \tag{4}$$

Eq. (4) shows that the path-averaged rainfall rate is proportional to the area under the time-lagged cross-covariance function of the rainfall-induced scintillation detected by two horizontally oriented line detectors with a vertical separation z_0.

The path-averaged number density of raindrops $\overline{N(a')}$ obtained from the space-time covariance function is (Wang *et al.*, 1977)

$$\overline{N(a')}\approx z_0^{-9}\tau^{10}C_\chi(z_0,\tau)g^{-3}(z_0/\tau)\times\left[g(z_0/\tau)+\frac{z_0}{\tau}\frac{g'(z_0/\tau)}{2}\right]^{-1}. \tag{5}$$

The mean drop size $\bar{D}$ can be obtained from the path-averaged number-density as

$$\bar{D}=2\int_0^\infty da a\overline{P(a)}, \tag{6}$$

where

$$\overline{P(a)}=\frac{\overline{N(a)}a^3v(a)}{\int_0^\infty da\overline{N(a)}a^3v(a)}. \tag{7}$$

An important assumption used in the derivation is that the time-lagged covariance function of the irradiance scintillation induced by many raindrops from different locations can be considered as the sum of the covariance functions of the scintillation pattern of each individual drop. This assumption is valid if the receiver detects only one diffraction pattern at a time. With a line detector, many patterns may be detected simultaneously and some of the irradiance scintillations will be cancelled. To see how much cancellation distorts the deduced rain rate and drop-size distribution, we performed a computer simulation (Wang and Lawrence, 1977). The simulation shows that, in practical cases, the cancellation results in a sizeable background correlation but no change in the shape of the covariance function. We can remove the background correlation by taking the difference between the covariance functions with positive and negative delays, i.e., $C_\chi(\tau)-C_\chi(-\tau)$. The path-averaged drop-size distribution and rain rate can still be obtained according to the previous analysis.

We have also assumed that the raindrops are spherical and this is not true for large drops. Our assumption has no significant effect on the drop-size measurement as long as we use a correct relationship between the terminal velocity and the drop diameter. Also, the oscillation of the raindrops will not affect the measurement because the detectors "see" many raindrops along the path simultaneously. The oscillation is random and produces no average effect.

3. Altitude correction

The empirical relationship between the terminal velocity and the drop size [Eq. (3)] given by Gunn and Kinzer (1949) was taken at sea level. In Colorado, this relationship must be corrected for altitude. Beard (1977) discussed a method for obtaining the terminal velocity of raindrops for different atmospheric conditions. Following his procedure we found that at Boulder, Colorado (altitude, 1.6 km MSL), the percent change of the terminal velocity from the sea level value is

$$\Delta v=9.3+1.1\ln D, \tag{8}$$

where D is the drop size (mm). The change of terminal velocity will also change $g(v)$ in Eq. (3) and hence the number density. However, for drop sizes in the region

from 0.8 to 5 mm, the effect is negligible. In the following results, we have used Eq. (8) for the altitude correction.

4. The instrument

Our prototype system consists of a laser transmitter, two line detectors and an analog correlator whose output feeds a computer that calculates precipitation quantities. A schematic diagram of the system is shown in Fig. 4. The transmitter is a 4 mW, He-Ne laser and optical collimator that produces a uniform beam 20 cm in diameter. The two receivers are horizontal linear detectors 25 cm long and 0.15 cm high with a variable vertical separation that is typically a few centimeters. To minimize interference from other light sources, filters exclude all light except a 0.002 μm passband centered at 0.6328 μm, and a telescope restricts the field of view to 2°. Correlation between the scintillations from the two receivers is accomplished in analog delay devices that multiply and integrate to obtain time-lagged covariance functions. As an option, the detected scintillation signals can be recorded by a stereo audio tape recorder controlled by an automatic switching device. A tipping-bucket raingage that sends a pulse to a chart recorder for each 0.254 mm of accumulated rainfall was located near the receiving end. The tape recorder was turned on by the first tip from the tipping-bucket raingage and turned off 20 min after the last tip. The recorded data then could be replayed for data processing.

5. Results

We operated our system in 1975 and 1976 at Boulder. More than 40 hr of precipitation data were recorded. Here we present the detailed analysis of three storms which occurred 28–29 May 1975, 23 June 1976 and 2 August 1976.

Light, steady rains lasted more than 7 h during 28–29 May 1975. The optical pathlength is 140 m for this measurement. From Eq. (4) the area under the covariance curve is proportional to the path-averaged rainfall rate. Fig. 5 compares these areas with the rain rates determined by the tipping-bucket gage. Because of the poor time-resolution of this gage in light rain, we averaged the optically measured rain rates between the successive tips. The agreement between the raingage and the optical measurements is good, with a correlation coefficient greater than 0.95.

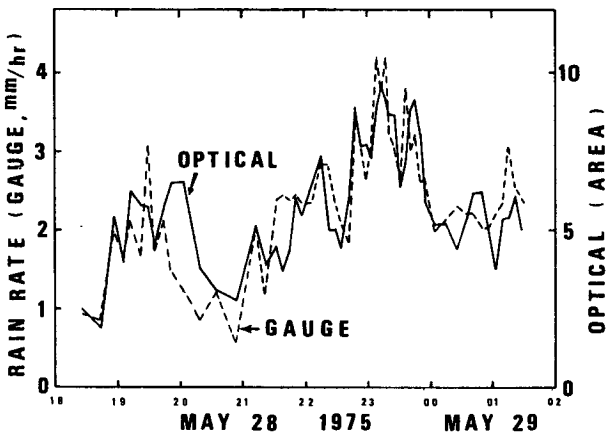

FIG. 5. The time variation of rain rates measured by a tipping-bucket raingage and by an optical raingage during steady rain on 28 and 29 May 1975.

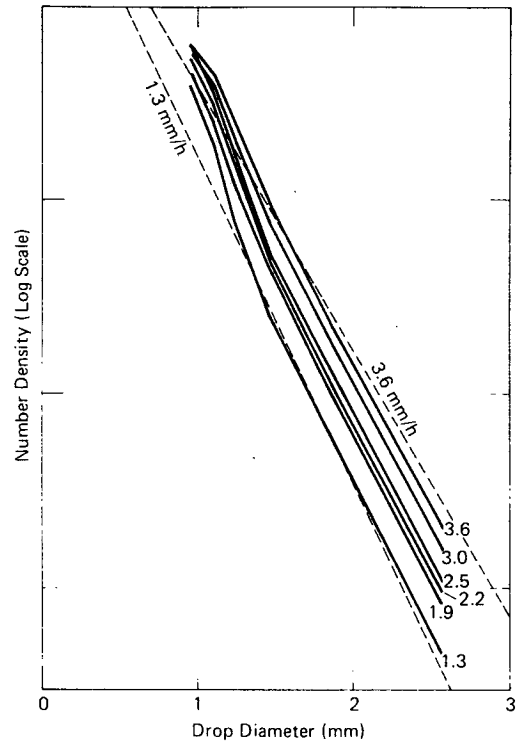

FIG. 6. The path-averaged raindrop size distribution versus the drop diameter for six groups of data divided according to the rainfall rate for the steady rain on 28–29 May 1975. The range of the number density of a Marshall-Palmer distribution is shown by the dashed lines.

The path-averaged raindrop number density versus the drop diameter [calculated from Eq. (1)] is shown in Fig. 6 for rain rates varying from 1.3 to 3.6 mm h^{-1}. Because we do not have the absolute number density in our measurements, we display the curves on an arbitrary vertical logarithmic scale. The corresponding range of the number density of a Marshall-Palmer distribution is shown by the dashed lines. The agreement between the number density deduced from the scintillation measurements and the empirical Marshall-Palmer distribution is good for this steady rain.

A bimodal velocity distribution was detected on 23 June 1976, during a mixture of rain and hail (pathlength, 200 m). The time-lagged covariance functions, each averaged over 5 min and taken with a slit spacing of 4 cm, are shown in Fig. 7. The peak at 4 ms contributed by hail-induced scintillations corresponds to a terminal velocity of 10 m s^{-1}. The 9 ms peak is caused by rain-

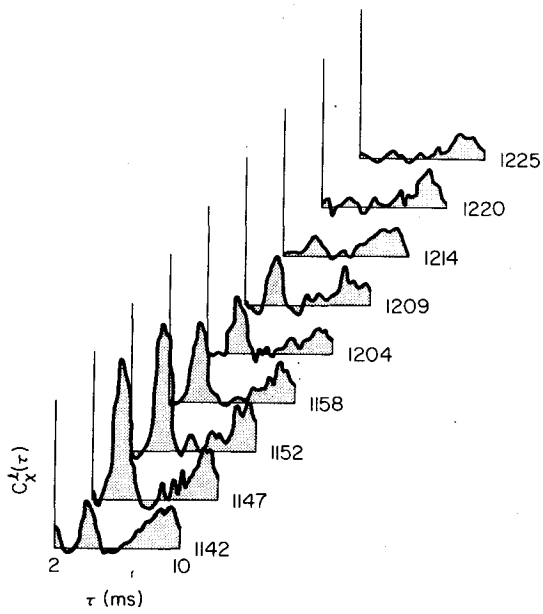

FIG. 7. The time-lagged covariance functions of the signals detected by two vertically separated line detectors with a separation of 4 cm on a 200 m path during a mixture of rain and hail on 23 June 1976.

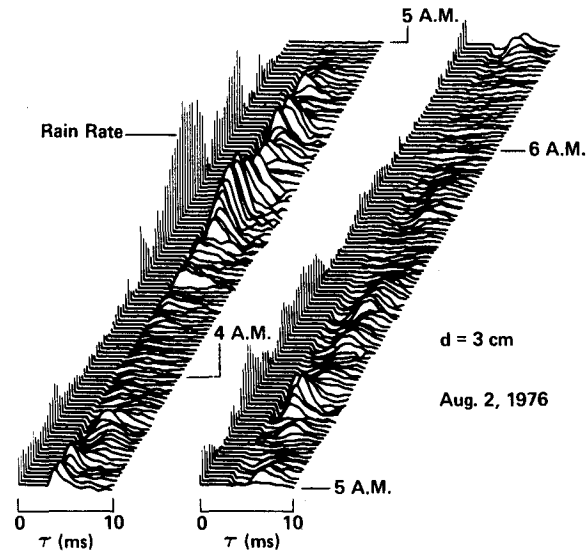

FIG. 9. The measured time-lagged covariance functions for every 42 s during the storm on 2 August 1976. The horizontal axis is the time lag in milliseconds. Total rain rate is indicated for each interval by the height of the vertical line at the left end of the covariance function. The flat portion leading each covariance function denotes the baseline.

drops with terminal velocity of 4.5 m s^{-1}. Near the end of the storm the hail disappeared while small raindrops were still falling. If we assume that the relationship between drop size and the terminal velocity follows that given by Gunn and Kinzer (1949), we obtain the drop-size distribution shown in Fig. 8. Because hail may not be presumed to follow the Gunn and Kinzer relationship, the values are only qualitatively correct for the hail sizes. The dashed lines represent the Marshall-Palmer drop-size distribution appropriate to the rain rate at that moment. Including the hail particles, the drop-size distributions have more large particles than a Marshall-Palmer distribution but at the end of the hail storm, the rainfall drop-size distribution agrees well with the Marshall-Palmer distribution.

Unfortunately, the raw scintillation signals detected by the two line detectors were not recorded for the previous two storms. Only time-lagged cross-covariance functions were recorded on either film or chart. As a re-

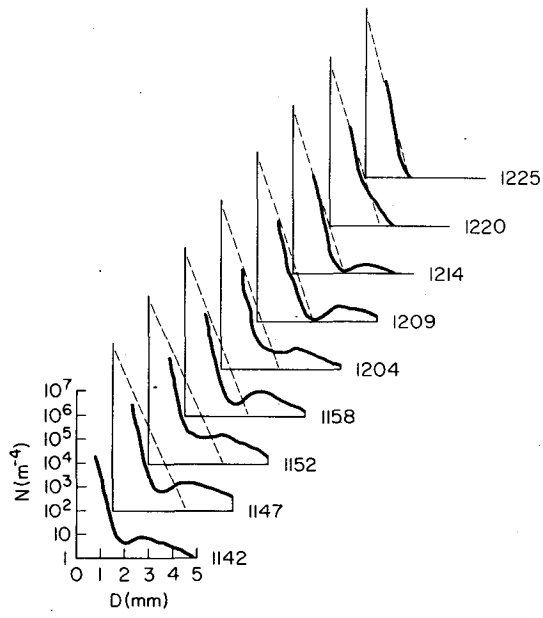

FIG. 8. The drop-size distribution of the signals detected by two vertically separated line detectors with a separation of 4 cm on a 200 m path during a mixture of rain and hail on 23 June 1976. The dashed lines indicate the corresponding Marshall-Palmer distribution appropriate to the rain rate at that moment.

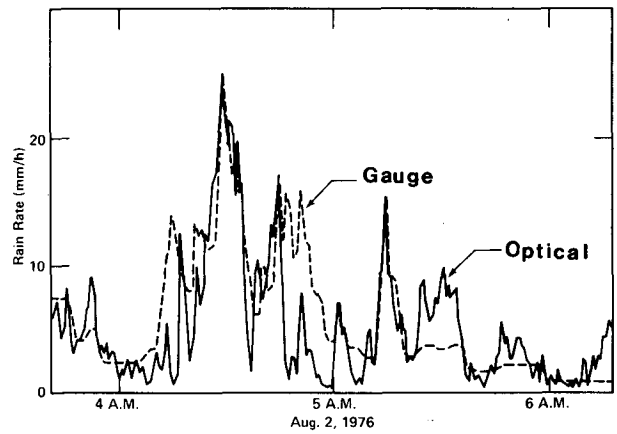

FIG. 10. A comparison between optically detected rain rates (solid line) and rain rates measured by a tipping-bucket raingage near the receiving end of the path (dashed line) for the storm on 2 August 1976.

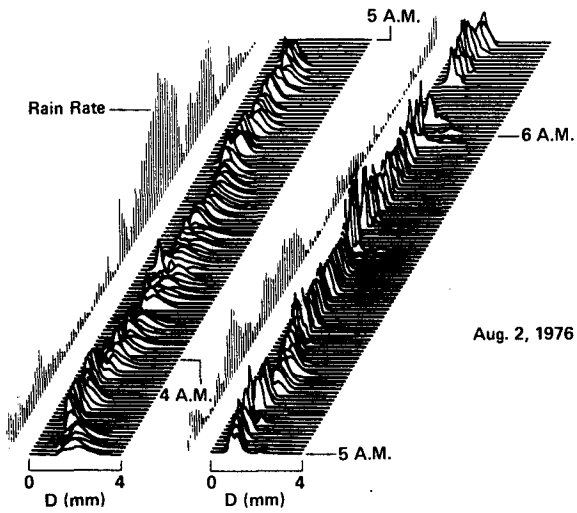

FIG. 11. The raindrop size distribution at 42 s intervals during the storm on 2 August 1976. The vertical axis is the relative fraction of rain rate contributed by drop-size intervals. The horizontal axis denotes the raindrop diameter. Total rain rate is indicated for each interval by the height of the vertical line at the left end of each distribution.

sult, a detailed analysis for the statistics of the drop-size distribution cannot be made for these data. For the storm on 2 August 1976, $2\frac{1}{2}$ h of raw signals were recorded. These recorded scintillations were later replayed through the analog correlator and the output time-lagged cross-covariance function was fed into a computer for detailed analysis.

The measured time-lagged covariance functions for every 42 s are shown in Fig. 9. The horizontal axis is the time lag in milliseconds. Total rain rate is also indicated for each interval by the height of the vertical line at the left end of each covariance function. The flat part leading each covariance function denotes the baseline. In retrieving the baseline, we took the difference between the covariance functions with positive and negative delays. From Eq. (4), the area under the covariance curve is proportional to the path-averaged rainfall rate. Fig. 10 compares these areas with rain rates determined by a tipping-bucket gage. The agreement is good but might have been better if readings of several raingages along the path could have been used. Raindrop size distributions for each 42 s interval are shown in Fig. 11. The vertical axis is the relative fraction of rain rate contributed by drop size intervals. The horizontal axis denotes the raindrop diameter. Total rain rate is indicated for each curve by the height of the vertical line at the left end of the distribution. Both the rain rate and the drop-size distribution changed rapidly during the storm. The heaviest rainfall tends to be correlated with large drop size except in the beginning of the storm when large drops occurred during rates of only 7 mm h^{-1}. Fig. 12 shows the mean raindrop size [obtained according to Eq. (6)] as a function of rain rate during the storm. The solid line shows the relation predicted by the Marshall-Palmer distribution. The scatter of experimental points is substantial for rain rates <10 mm h^{-1}, whereas a linear relationship falling somewhat below the Marshall-Palmer line is evident for higher rates.

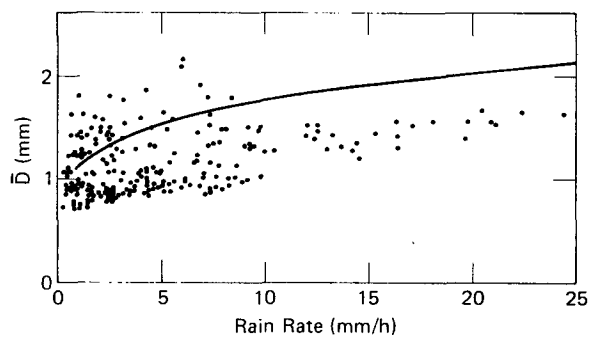

FIG. 12. The mean raindrop size as a function of rain rate for the storm of 2 August 1976. The solid line indicates the mean drop size of the Marshall-Palmer distribution.

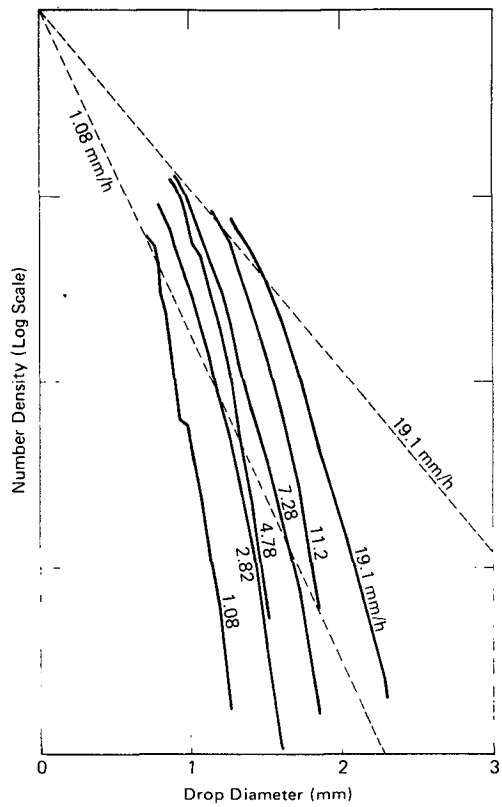

FIG. 13. The path-averaged raindrop size distribution as a function of drop diameter for six groups of data divided according to the rainfall rate on 2 August 1976. The range of the number density of a Marshall-Palmer distribution is shown by the dashed lines.

The path-averaged raindrop number density [from Eq. (5)] versus the drop diameter is shown in Fig. 13 for rain rates varying from 1.08 to 19.1 mm h^{-1}. The corresponding range of the number density of a Marshall-Palmer distribution is shown by the dashed lines.

Contrary to the number density of the steady rain on 28–29 May 1975 (Fig. 6), the raindrop size of this storm is smaller than the empirical Marshall-Palmer distribution.

6. Conclusions

We have demonstrated an optical device that measures path-averaged rainfall rate and drop-size distribution. The technique has the following advantages: 1) the measured quantities are path-averages and do not depend on variations whose spatial scale is smaller than the optical path length; 2) prior knowledge of the drop-size distribution is not required to obtain total rainfall rate; 3) the actual path-averaged drop size distribution can be measured; and 4) because spatial integration (path averaging) is used, time resolution as short as 20 s is possible.

The measured drop-size distribution changes rapidly during a storm and varies from storm to storm. The heaviest rainfall tends to be correlated with larger drop size. However, the scatter of measured mean drop size is substantial for light rain rate (<10 mm h^{-1}). The raindrops may not follow the empirical Marshall-Palmer distribution, especially at the beginning of a storm when large drops often occurred with low rain rates.

Acknowledgment. We would like to thank an anonymous reviewer for suggesting the use of the approach developed by K. V. Beard (1977) for altitude correction.

REFERENCES

Arnulf, A., and J. Bricard, 1957: Transmission by haze and fog in the spectral region 0.35–10 microns. *J. Opt. Soc. Amer.*, **47**, 491–498.

Atlas, D., 1953: Optical extinction by rainfall. *J. Meteor.*, **10**, 486–488.

——, and C. W. Ulbrich, 1974: The physical basis for attenuation-rainfall relationships and the measurement of rainfall parameters by combined attenuation and radar methods. *J. Rech. Atmos.*, **8**, 275–298.

——, and C. W. Ulbrich, 1976: Path and area-integrated rainfall measurement by microwave attenuation in the 1–3 cm band. *Preprints 17th Radar Meteorology Conf.*, Seattle, Amer. Meteor. Soc., 1–8.

Beard, K. V., 1977: Terminal velocity adjustment for cloud and precipitation drops aloft. *J. Atmos. Sci.*, **34**, 1293–1298.

Chu, T. S., and D. C. Hogg, 1966: The attenuation of 3.392 μ He-Ne laser radiation by methane in the atmosphere. *Bell Sys. Tech. J.*, **45**, 301–306.

——, and D. C. Hogg, 1968: Effects of precipitation on propagation at 0.63, 3.5 and 10.6 microns. *Bell Sys. Tech. J.*, **47**, 723–759.

Gunn R., and G. D. Kinzer, 1949: The terminal velocity of fall for water droplets in stagnant air. *J. Meteor.*, **6**, 243–248.

Hogg, D. C., and T. S. Chu, 1975: The role of rain in satellite communications. *Proc. IEEE*, **63**, 1308–1331.

Marshall, J. S., and W. McK. Palmer, 1948: The distribution of raindrops with size. *J. Meteor.*, **5**, 165–166.

Van de Hulst, H. C., 1957: *Light Scattering by Small Particles.* Wiley (see pp. 103–113).

Wang, Ting-i, and S. F. Clifford, 1975: Use of rainfall-induced optical scintillations to measure path-averaged rain parameters. *J. Opt. Soc. Amer.*, **65**, 927–937.

——, and K. B. Earnshaw, 1977: An optical velocimeter for precipitation. *Topical Meeting on Optical Propagation through Turbulence, Rain, and Fog*, Boulder, Opt. Soc. Amer., ThB5 1–4.

——, and R. S. Lawrence, 1977: Measurement of rain parameters by optical scintillation: computer simulation of the correlation method. *Appl. Opt.*, **16**, 3176–3179.

——, K. B. Earnshaw, and R. S. Lawrence, 1978: Simplified optical path-averaged rain gauge. *Appl. Opt.*, **17**, 384–390.

——, G. Lerfald, R. S. Lawrence and S. F. Clifford, 1977: Measurement of rain parameters by optical scintillation. *Appl. Opt.*, **16**, 2236–2241.

Wilson, R. W., and A. A. Penzias, 1966: Effect of precipitation on transmission through the atmosphere. *Nature*, **211**, 1081.